

Skin-Friction and Forced Convection from an Isothermal Rough Plate

Aubrey G. Jaffer
e-mail: agj@alum.mit.edu

Abstract

A novel analysis of the turbulence generated by flow over self-similar roughness yields new correlations for total skin-friction coefficient and forced convection from both self-similar and self-dissimilar isothermal plates having root-mean-squared (RMS) height-of-roughness ε :

$$f_c = \frac{1}{3 \ln^2(L/\varepsilon)} \quad \text{Nu} = \frac{\text{Re Pr}^{1/3}}{6 \ln^2(L/\varepsilon)}$$

An analysis of Nikuradse’s original sand-roughness data yields a RMS roughness to sand-roughness conversion factor of 5.385, which is within 1% of the 5.333 conversion factor fit by Afzal, Seena, and Bushra. When corrected for a scaling error in Nikuradse’s original experiments, the formulas from both Prandtl and Schlichting and Mills and Hang are in agreement with the new skin-friction coefficient formula in “the completely rough regime” (large Reynolds numbers).

This new theory differs from Prandtl and Schlichting in the transitional rough regime. The new formulas predict that the skin-friction coefficient will have no dependence on Reynolds number, and that forced convection will have a linear dependence on Reynolds number. Convection measurements of a self-dissimilar plate having precisely 3 mm of RMS roughness match the linear correlation within 3% at Reynolds numbers from 5500 to 50000.

Keywords: turbulence; skin-friction; profile roughness; sand-roughness; forced-convection

Table of Contents

<i>Introduction</i>	2
<i>Prior Work</i>	3
<i>Roughness</i>	4
<i>Self-Similar Profile Roughness</i>	5
<i>Self-Similar Surface Roughness</i>	6
<i>Vertical Roughness Travel</i>	7
<i>Skin-Friction and Forced Convection</i>	9
<i>Self-Dissimilar Roughness</i>	9
<i>Physical Measurements</i>	10
<i>Transitional Rough Regime</i>	11
<i>Sand-Roughness</i>	12
<i>Roughness in Pipes</i>	14
<i>Conclusions</i>	15
<i>Nomenclature</i>	15
<i>References</i>	16

arXiv:1810.05743v3 [physics.flu-dyn] 25 Jun 2019

1. Introduction

Predicting the skin-friction of a rough surface is important to the fluid dynamics of vehicles and turbines. The related phenomenon of forced convection from a rough surface has application to modeling weather and the thermal behavior of buildings.

Skin-friction of a plate with a rough surface is different in character from skin-friction of a smooth flat surface because the peaks of roughness protrude through what would otherwise be a laminar boundary-layer adjacent to the plate.

Prandtl and Schlichting[1] assert that the plate’s height-of-roughness decreases relative to the depth of the boundary-layer growing along the plate in the direction of flow. This would not be true of a surface with self-similar roughness (as defined in Section 3). The ratio of the height-of-roughness to the characteristic-length of the plate being constant means that the height-of-roughness grows linearly with plate length (from its leading edge). Laminar and smooth-turbulent boundary layers grow proportionally to $x^{1/2}$ and $x^{4/5}$ respectively; the self-similar height-of-roughness grows faster ($\propto x^1$) than both; thus its whole length sheds rough turbulence.

Prandtl and Schlichting split their analysis into three regions based on boundary-layer depth. For the present work, self-similarity requires only a single analysis which does not use boundary-layer theory.

Another contention with prior work is that turbulent skin-friction can occur adjacent to plates under isobaric conditions; but flow in pipes is not isobaric.¹ Prandtl and Schlichting applied the methods of pipe flow analysis to rough plates; the present work does not, although conversions between roughness metrics appear to work the same for pipes and plates.

Section 2 describes prior work and demonstrates a scaling problem with the legacy “sand-roughness” metric.

Section 3 defines profile and surface roughness, the root-mean-squared (RMS) height-of-roughness metric, and a type of self-similarity for profile roughness functions.

Section 4 gives three examples of discrete self-similar profile roughness functions.

Section 5 shows the surfaces generated by summing each discrete profile function with itself rotated 90°.

Section 6 derives a single formula for the total vertical travel of a conforming flow for two of the discrete profile roughness functions from Section 4. The ratio of vertical roughness travel to horizontal travel is used to scale the bulk fluid velocity to the “roughness velocity”.

Section 7 formulates the skin-friction coefficient as the square of the ratio of roughness velocity to bulk fluid velocity.

Section 8 considers the new theory’s application to rough surfaces which lack self-similarity (are “self-dissimilar”).

Section 9 evaluates the new convection formula on a bi-level, self-dissimilar plate and finds that convection measurements of the plate match the new formula within 3% at Reynolds numbers (Re) from 5500 to 50000.

Section 10 discusses the behavior of rough plates at low Re. The present work’s prediction of constant skin-friction coefficient is indirectly confirmed from convection measurements of the bi-level (self-dissimilar) plate. Section 12 discusses the implications for roughness in pipes.

Section 11 examines the sand-roughness metric and its relation to the RMS roughness metric, enabling comparisons with prior works, which are presented.

¹ Skin-friction causes pressure loss in flow through the pipe.

2. Prior Work

In 1934 Prandtl and Schlichting published *Das Widerstandsgesetz rauher Platten (The Resistance Law for Rough Plates)*[1], which brilliantly infers a relation for skin-friction resistance for rough plates from their analysis of Nikuradse’s measurements of sand glued inside pipes. In *Boundary-layer theory*[2] Prandtl and Schlichting give a formula for fully rough (large Re) total skin-friction coefficient for a rough flat plate:

$$c_f = \left(1.89 + 1.62 \log_{10} \frac{L}{k_S}\right)^{-2.5} \quad 10^2 < L/k_S < 10^6 \quad (1)$$

In *On the Skin Friction Coefficient for a Fully Rough Flat Plate*[3], Mills and Hang present a formula which they claim to be more accurate on the local skin-friction measurements done by Pimenta, Moffat, and Kays[4]. The corrected² total skin-friction formula is:

$$C_D = \left(2.035 + 0.618 \ln \frac{L}{k_S}\right)^{-2.57} \quad (2)$$

The roughness in both articles is reported in Nikuradse’s sand-roughness metric k_S , the height of “coarse and tightly placed roughness elements such as for example coarse sand grains glued on the surface”. Prandtl and Schlichting[1] gives the parameters of Nikuradse’s sand coatings, which are reproduced as the left two columns in Table 1.

k_S	grains/cm ²	k_S^{-2}
.08 cm	150	156.25/cm ²
.04 cm	590	625/cm ²
.02 cm	1130	2500/cm ²
.01 cm	4600	10000/cm ²

Table 1 Nikuradse’s sand coatings

Because their packing densities scale as the inverse squared of grain size, the .08 cm and .04 cm sand coatings should scale correctly as long as the glue thickness is proportional to grain size. Similarly the .02 cm and .01 cm sand coatings should scale.

The two coarsest coatings (largest k_S values) had packing densities slightly less than a square packing. The other two had packing densities less than half that of a square packing. But comparing the .02 cm and .04 cm sand coatings, their packing density ratio is nearly 1:2, not 1:4. Thus formulas (1) and (2) will have incorporated a scale error (between measurements of large and small k_S) and should not be applied to L/k_S values much larger than 1000 (507 is the largest rough pipe L/k_S value in Schlichting[2] Fig. 20.18). Section 11 compares these formulas with the present work.

² Mills and Hang’s published formula had a “6” where a “0” should have been in the first constant:

$$C_D = \left(2.635 + 0.618 \ln \frac{L}{k_S}\right)^{-2.57}$$

All of their measurement comparisons were of local skin-friction, which used a different formula. Their only use of the total skin-friction formula was a comparison with the Prandtl and Schlichting formula, which overstated the magnitude and negated the sign of that difference because of the error. Figure 11 shows traces for both the corrected and uncorrected formulas.

3. Roughness

Profile roughness is a function $z(x)$ where $0 \leq x \leq L$ is distance from the leading edge in the direction of flow.

Surface roughness is a function $z(x, y)$ of the x and y coordinates in the surface of the plate. There are no tunnels or overhangs. In order that the random fluid velocities resulting from interaction with the plate roughness are not skewed, $z(x, y)$ should be roughly isotropic; swapping x and y should not materially affect the behavior of the system. A surface composed of parallel ridges and valleys would not meet this criterion.

Consider the roughness profile $z(x)$ for a plate cut into strips parallel to the flow, each strip L long. The mean height \bar{z} and root-mean-squared height-of-roughness ϵ of the strip are:

$$\bar{z} = \frac{1}{L} \int_0^L z(x) dx \quad \epsilon = \sqrt{\frac{1}{L} \int_0^L [z(x) - \bar{z}]^2 dx} \quad (3)$$

The mean height \bar{z} and root-mean-squared height-of-roughness ϵ of surface roughness are:

$$\bar{z} = \frac{1}{L^2} \int_0^L \int_0^L z(x, y) dx dy \quad \epsilon = \sqrt{\frac{1}{L^2} \int_0^L \int_0^L [z(x, y) - \bar{z}]^2 dx dy} \quad (4)$$

These roughness functions need not be continuous to be integrable. Local flow properties may not be well-defined anywhere. The present analysis is of total skin-friction over the strip.

A profile roughness function $z(x)$ has self-similar roughness with (integer) branching factor $n > 0$ if the RMS height-of-roughness of $z(x)$ over an interval $x_0 < x < x_n$ is n times the RMS height-of-roughness of $z(x)$ over each (evenly divided) sub-interval $x_j < x < x_{j+1}$ for $0 \leq j < n$ at a succession of scales converging to 0.

Note that $z(x_j)$ values contribute to the interval height-of-roughness, but not to any sub-interval height-of-roughness.

If profile roughness function $z(x)$ has self-similar roughness, then the ratio of the length of the interval L to its RMS height-of-roughness ϵ will be invariant over that succession of scales converging to 0.

Self-similarity is of interest because the skin-friction coefficient f_c , which will be formulated in Section 7, is a function of L/ϵ . If the roughness is self-similar, then L/ϵ and $f_c(L/\epsilon)$ will be constant over the span of the roughness profile.

In the three examples of self-similar profile roughness in Section 4, the roughness function is simply a permutation of the linear ramp $z(x) = x$ from $x = 0$ to $x = w$. Because the RMS height-of-roughness calculation depends only on the z values and not their relation to x , for all ramp-permutation profile roughness:

$$\epsilon = \sqrt{\frac{1}{w} \int_0^w [x - w/2]^2 dx} = \frac{w}{\sqrt{12}} \quad (5)$$

This leads to the question of whether a linear ramp, which is a permutation of a linear ramp, can cause turbulence. While vortexes can arise in two-dimensional flows, turbulence is a three-dimensional phenomena. The random velocity fluctuations must be isotropic at all but the coarsest length scales. Not only must the height profile be rough in the direction of flow, but perpendicular to the flow as well. This rules out simple ramps as roughness profiles.

A linear ramp being disqualified, are self-similar roughness profiles possible?³ Section 4 constructs three examples of self-similar roughness profiles.

³ Flack, Schultz, Barros, and Kim[5] remark that the shape of the roughness function (ΔU^+) for all fifteen of their grit-blasted surfaces shows self-similarity.

4. Self-Similar Profile Roughness

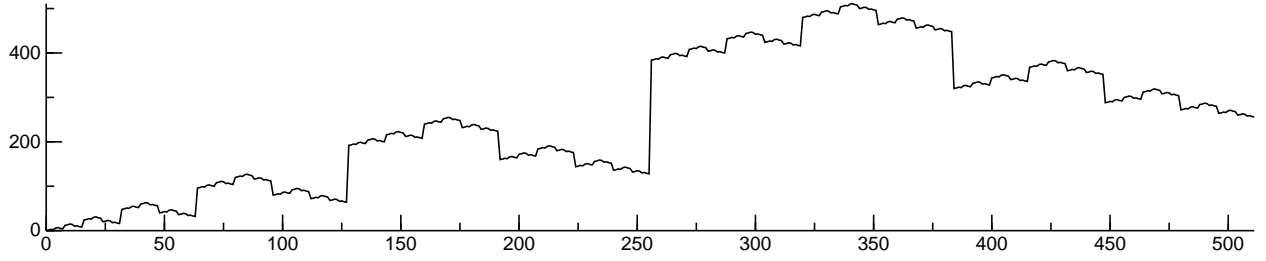


Figure 1 Gray-code profile roughness

The integer Gray-code sequence $G(x, w)$ with $0 \leq x < w = 2^j$ shown in Figure 1 has a RMS height-of-roughness $\epsilon = w/\sqrt{12}$ from equation (5) and is a self-similar roughness (when bisected) as seen by its recurrence:

$$G(x, w) = \begin{cases} x, & \text{if } w = 1; \\ w + G(w - 1 - (x \bmod w), w/2), & \text{if } \lfloor x/w \rfloor = 1; \\ G(x \bmod w, w/2), & \text{otherwise.} \end{cases} \quad (6)$$

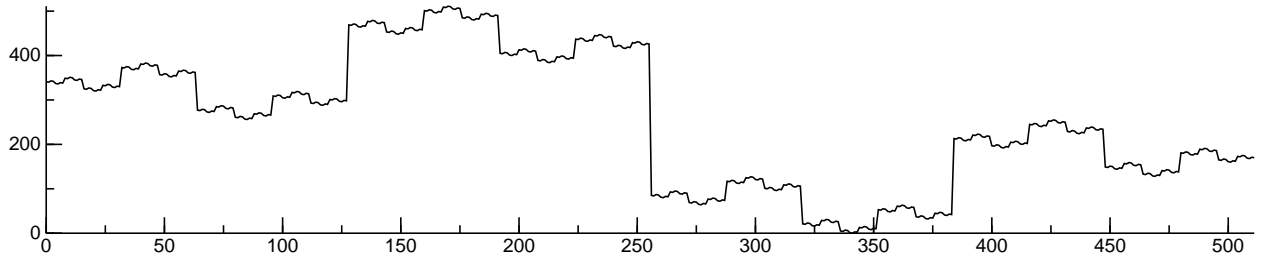


Figure 2 Wiggliest self-similar profile roughness

The integer sequence $W(x, w)$ which reverses at each bifurcation produces the wiggliest possible self-similar roughness with $0 \leq x < w = 2^j$ and is shown in Figure 2; it has a RMS height-of-roughness $\epsilon = w/\sqrt{12}$:

$$W(x, w) = \begin{cases} x, & \text{if } w = 1; \\ \lfloor x/w \rfloor w + W(w - 1 - (x \bmod w), w/2), & \text{otherwise.} \end{cases} \quad (7)$$

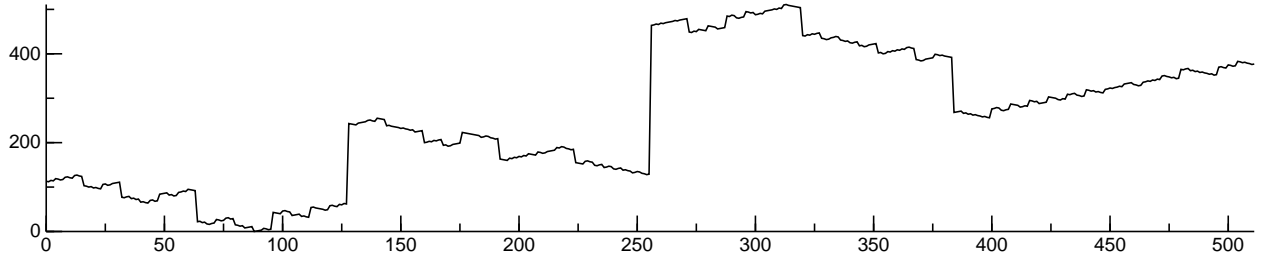


Figure 3 Randomly reversing bifurcation profile roughness

Figure 3 shows an integer sequence generated by recursive-descent with random reversing at each halving. It has a RMS height-of-roughness $\epsilon = w/\sqrt{12}$; its roughness is approximately self-similar.

5. Self-Similar Surface Roughness

A $L \times L$ self-similar roughness function $z(x, y)$ can be constructed from a profile roughness function $Y(x, w)$:

$$z(x, y) = \frac{\varepsilon \sqrt{6}}{w} \left[Y\left(x \frac{w}{L}, w\right) + Y\left(y \frac{w}{L}, w\right) \right] \quad w = 2^j$$

When the profile roughness is a linear ramp permutation, the surface height-of-roughness ε is $\sqrt{2}$ times the profile height-of-roughness ϵ .

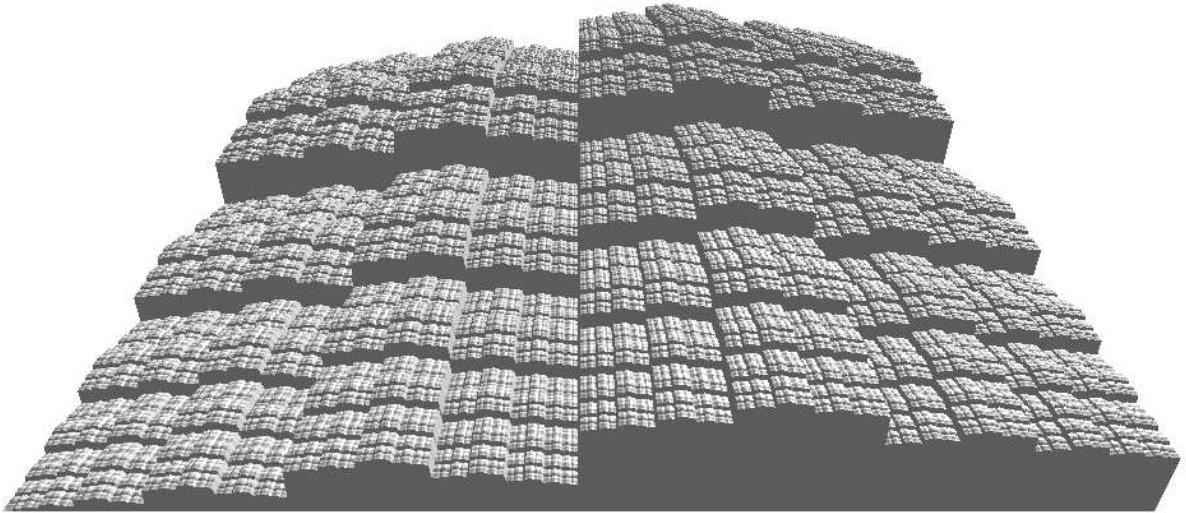


Figure 4 Gray-code surface roughness

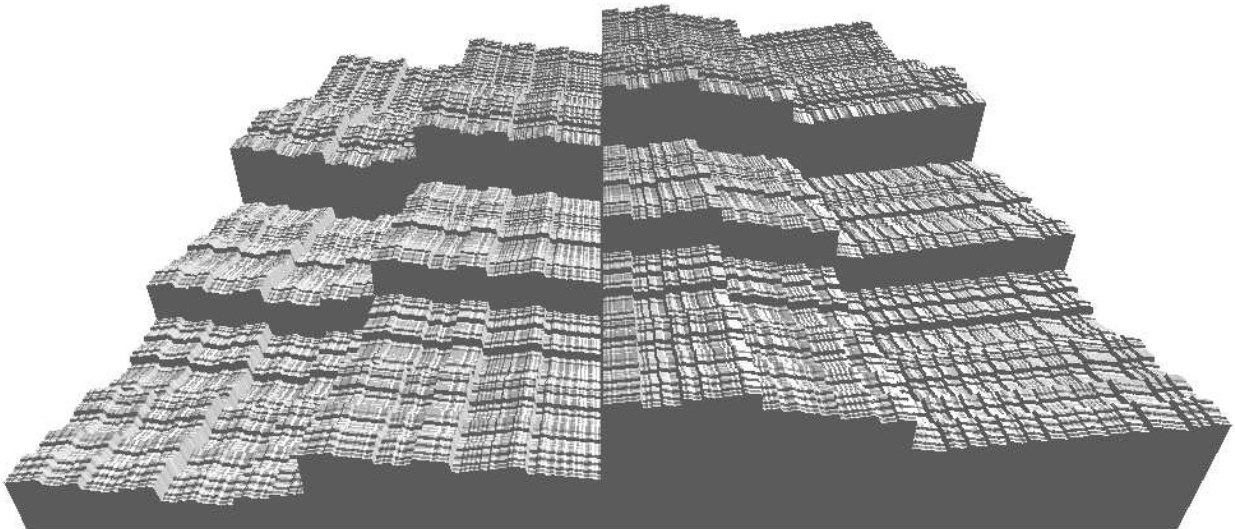


Figure 5 Randomly reversing bifurcation surface roughness

Figures 4 and 5 show squared Gray-code and random-roughness corresponding to Figures 1 and 3 respectively. These look like faulted and weathered granite outcroppings.

Figure 6 shows squared wiggly roughness corresponding to Figure 2. Unnatural in appearance, it resembles tire treads.

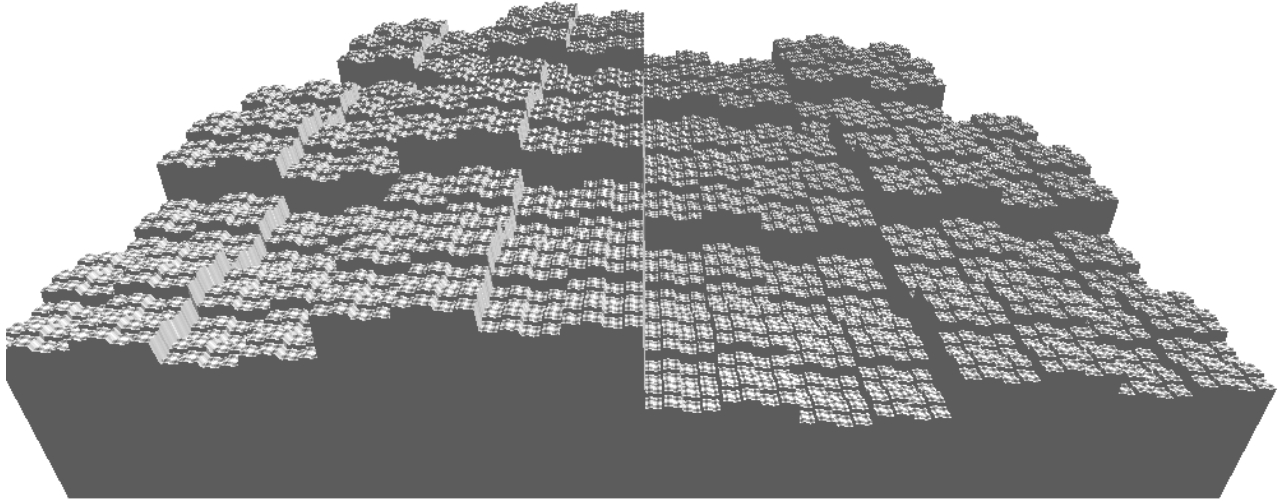


Figure 6 Wiggliest self-similar surface roughness

6. Vertical Roughness Travel

For roughness profile $Y(x, w)$, the sum of the lengths of all horizontal segments is $w - 1 = 2^j - 1$. The sum of the absolute value of the length of each vertical segment is:

$$\sum_{x=0}^{2^j-2} |Y(x, 2^j) - Y(x+1, 2^j)| \quad (8)$$

If a point were to trace a roughness profile $Y(x, w)$ from $x = 0$ to $x = w - 1$, then $w - 1$ is the horizontal distance it would travel, while formula (8) is the vertical distance.

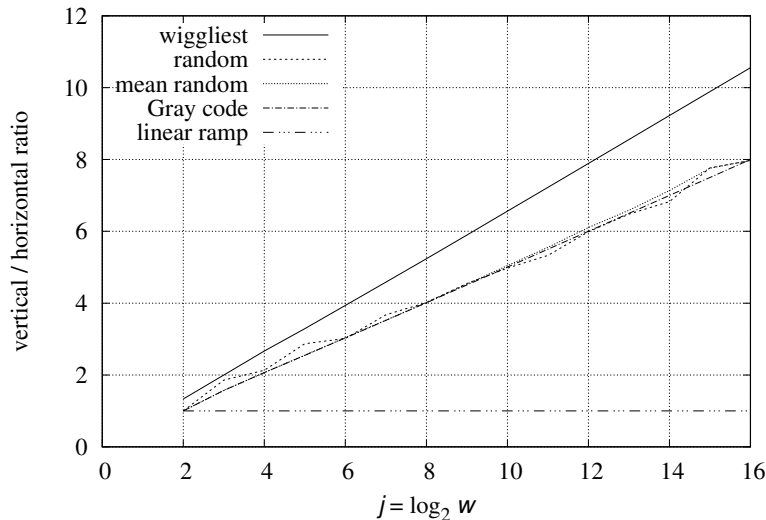


Figure 7 Vertical travel of roughness

Shown in Figure 7 is the vertical to horizontal travel ratio versus j , the base-2 logarithm of w . While the slope of $1/2$ is the same for the Gray-code and random cases, it is $2/3$ for the wiggliest roughness W . And the vertical segments in Figure 2 are indeed longer than the vertical segments in Figures 1 and 3.

Wiggliest roughness profile $W(x, w)$ is an extreme case; it reverses vertical direction at each increment of x . For each wiggliest roughness profile there are many more random bifurcation roughness profiles. Going forward $W(x, w)$ will be ignored as an outlier.

From Figure 7 the vertical to horizontal travel ratio for the Gray-code and random sequences is close to:

$$\frac{j}{2} = \frac{\log_2 w}{2} \quad (9)$$

Formula (9) is unbounded as w increases. At some scale of w , vertical fluid movement by a distance of L/w will induce negligible turbulence. The argument to \log_2 must be dimensionless. $\log_2(\epsilon/L)$ is always negative because $\epsilon \ll L$; $\log_2(L/\epsilon)$ is positive, but inverts the sense of formula (9). Letting $w = L/\epsilon$, the ratio of vertical to horizontal travel is then:

$$\frac{2}{\log_2(L/\epsilon)} \quad (10)$$

The maximum peak-to-valley height is $\sqrt{12}$ times the RMS height-of-roughness ϵ . So the vertical to horizontal ratio should be scaled:

$$\frac{1}{\sqrt{12}} \frac{2}{\log_2(L/\epsilon)} = \frac{1}{\sqrt{3} \log_2(L/\epsilon)} \quad (11)$$

In *Self-Similar Processes Follow a Power Law in Discrete Logarithmic Space*[6] Newberry and Savage demonstrate that some self-similar systems which are often modeled using continuous power-law probability distributions (such as the Pareto distribution) are better modeled using discrete power-law distributions.

The present work uses their idea in reverse. Conversion of flow into turbulence by contact with discrete self-similar roughness having been derived above, the turbulence generation by a continuous self-similar roughness will be inferred using a random variable.

The base-2 logarithm is an artifact of the discrete roughness functions from Section 4. The analogous mean field theory is to treat $Z = |\Delta Y|$ as a continuous random variable having a Pareto distribution where the frequency of Z is inversely proportional to Z^2 :

$$1 / \left[\int_{\epsilon}^L \frac{\sqrt{3} Z}{Z^2} dZ \right] = \frac{1}{\sqrt{3} \ln(L/\epsilon)} \quad (12)$$

Note that the surface height-of-roughness ϵ is used in equation (12) instead of the profile height-of-roughness ϵ in (11).

7. Skin-Friction and Forced Convection

For a rough flat surface subjected to a steady flow parallel to its surface which is sufficiently fast to generate turbulence, the skin-friction drag is the pressure opposing the flow due to viscous dissipation of that turbulence. As the height of roughness ε grows relative to the characteristic-length L , pressure drag (which is not dissipative) grows. $L/\varepsilon \gg 1$ constrains the system so that skin-friction drag dominates pressure drag.

The skin-friction coefficient f_c is the ratio of the shear stress τ , which is the skin-friction drag in this case, to the flow's kinetic energy density $\rho u^2/2$.

$$f_c = \frac{\tau}{\rho u^2/2} \quad (13)$$

f_c is dimensionless; both τ and $\rho u^2/2$ have units of pressure, kg/(m s²).

Scaling by the vertical to horizontal travel ratio from formula (12) converts a horizontal velocity u to a vertical roughness velocity u_R , from which τ is derived:

$$u_R = \frac{u}{\sqrt{3} \ln(L/\varepsilon)} \quad \tau = \frac{\rho u_R^2}{2} = \frac{\rho u^2}{6 \ln^2(L/\varepsilon)} \quad (14)$$

Combining equations (14) and (13) produces a formula for f_c dependent only on L/ε :

$$f_c = \frac{1}{3 \ln^2(L/\varepsilon)} \quad (15)$$

Figure 11 plots f_c over four decades of L/ε .

The Chilton and Colburn J-factor analogy (16) relates friction factors to turbulent forced convective heat transfer.

$$\text{Nu} = \frac{f_c}{2} \text{Re Pr}^{1/3} \quad (16)$$

Combining equation (16) with equation (15) produces a correlation for forced convection:

$$\text{Nu} = \frac{\text{Re Pr}^{1/3}}{6 \ln^2(L/\varepsilon)} \quad (17)$$

8. Self-Dissimilar Roughness

What can be learned from physical measurements of skin-friction or forced-convection from rough plates?

If a plate with a discrete self-similar roughness profile were measured and had the predicted dependence on Re , it could confirm the correlations for a very limited class of roughness. If a plate with a continuous self-similar roughness were tested, then the class would be larger, but still restricted to self-similarity. If measurements (at multiple Re values) of a self-dissimilar plate were to conform to the new convection correlation (as is revealed in Section 9), then that would be strong evidence that the new correlations reflect a physical law of turbulent isobaric flow over surface roughness.

The roughness metric conversions found in Section 11 extend the applicability of the new correlations to plates with a specified sand-roughness.

9. Physical Measurements

The Convection Machine[7] bi-level plate surface was composed of (676) $8.28 \text{ mm} \times 8.28 \text{ mm} \times 6 \text{ mm}$ posts spaced on 11.7 mm centers. The area of the top of each post is 0.686 cm^2 , half of the 1.37 cm^2 cell. The root-mean-squared height-of-roughness was 3 mm. This bi-level architecture provides the roughest surface possible in a 6 mm peak-to-valley span. And this plate surface has no self-similarity.⁴

Applying formula (17) yields $\text{Nu} = 0.0078 \text{ Re Pr}^{1/3}$. The corresponding trace “Rough Turbulent Asymptote” in Figure 8 matches the “ $\Delta T=11\text{K}$ Measured” convection within $\pm 3\%$ from $\text{Re} = 5500$ to 50000 .⁵

This is strong evidence that formulas (15) and (17) are intrinsic to turbulent isobaric flow over roughness and not specific to self-similar roughness profiles. The factor of $1/3$ in formulas (15) and (17) derive from $\sqrt{12}$ in equation (5). That is strong evidence that root-mean-squared height-of-roughness is the correct metric for roughness.

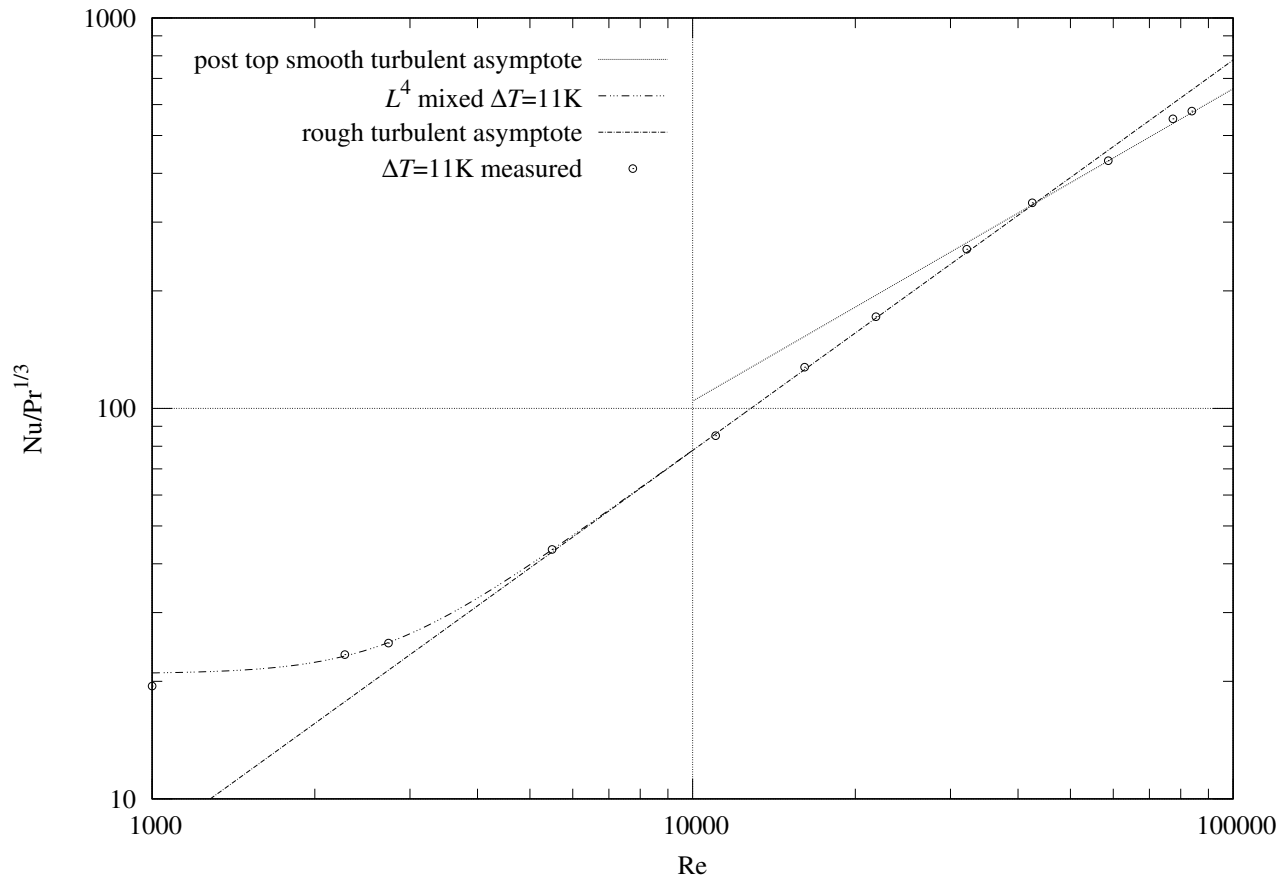


Figure 8 Convection from rough plate

⁴ Self-similarity is similarity between shape at different scales; but these blocks are all the same size.

⁵ In Figure 8 at $\text{Re} < 5500$ the “ L^4 mixed $\Delta T=11\text{K}$ trace for equation (17) is corrected for mixed convection, as described in *Turbulent Mixed Convection from an Isothermal Plate*[8]. At $\text{Re} > 50000$ the “post top smooth turbulent asymptote” trace shows that convection is mostly from the smooth post tops and no longer behaving as equation (17).

10. Transitional Rough Regime

Afzal, Seena, and Bushra[9] (and Schlichting[2]) relate that the internal roughness of commercial pipes behaves differently from Nikuradse’s sand coated pipes. While the curves for commercial pipes are monotonically decreasing on the Moody diagram, the diagram for Nikuradse’s pipes are not monotonic, which they term “inflectional”. Prandtl and Schlichting’s plate model apparently inherited the inflectional curve from Nikuradse’s pipes. The total coefficient of resistance (c_f) Moody diagram from Prandtl and Schlichting[1] shows a 10% dip spread over one and a half decades of Re just to the right of the smooth skin-friction line for each horizontal trace.

For a self-similar roughness (producing turbulence) there should be no variation in skin-friction coefficient with Reynolds number.

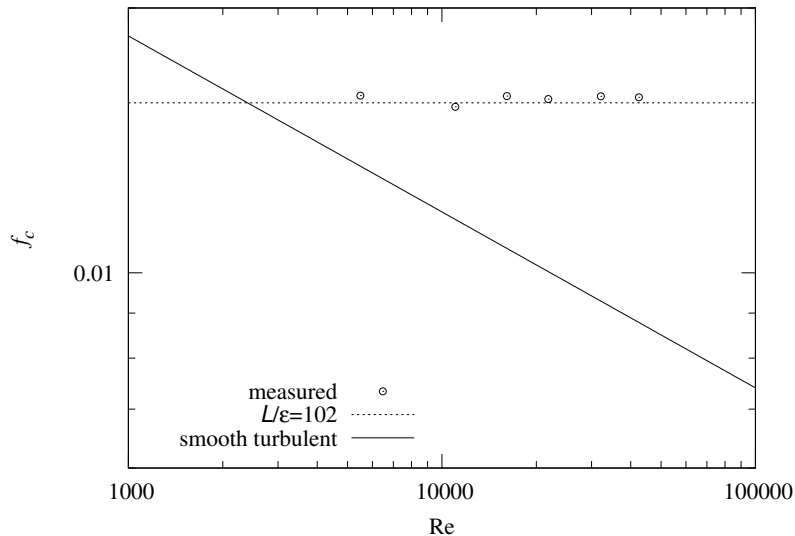


Figure 9 f_c vs. Re for bi-level plate

Figure 9 is a Moody diagram of the 3 mm RMS roughness bi-level plate measurements converted to friction coefficients f_c using the Chilton and Colburn J-factor analogy (16). The “measured” points hew closely to the “ $L/\varepsilon = 102$ ” line at $f_c = 0.0156$ and are flat within the expected measurement uncertainties.⁶

That the roughest possible surface, which is self-dissimilar, behaves like a self-similar surface in having no dependence on Re is strong evidence that correlation (15) applies over a wide range of turbulent flow. This independence of Re contrasts with rough pipe interiors and Prandtl and Schlichting’s[1] theory, where f_c depends on Re except in “the completely rough regime”. The implications for pipes are discussed in Section 12.

⁶ Convection at $Re < 5500$ is mixed with natural convection for which the analogy doesn’t apply.

11. Sand-Roughness

Modeling sand grains as unit radius spheres glued to the plate surface in a square array and modeling the space not covered by a sphere as glue of height $0 \leq \bar{g} \leq 1$, the mean height of the enclosing square cell of area A containing a unit sphere is:

$$\bar{z} = \left(\int_0^1 2\pi x (\sqrt{1-x^2} + 1) dx + (A - \pi)\bar{g} \right) / A = \left(\frac{5}{3}\pi + (A - \pi)\bar{g} \right) / A$$

The (dimensionless for unit radius sphere) root-mean-squared height-of-roughness R_q is:

$$2 R_q = \sqrt{\left(\int_0^1 2\pi x (\sqrt{1-x^2} + 1 - \bar{z})^2 dx + (A - \pi)(\bar{z} - \bar{g})^2 \right) / A}$$

For glue level $1 < \bar{g} < 2$, the grains are more than 50% submerged. Let $r_g = \sqrt{(1 - (\bar{g} - 1)^2)} = \sqrt{2\bar{g} - \bar{g}^2}$ be the radius of the glue opening through which the sphere is exposed. The mean height of the enclosing square cell of area A containing a unit sphere is then:

$$\bar{z} = \left(\int_0^{r_g} 2\pi x (\sqrt{1-x^2} + 1) dx + (A - \pi r_g^2)\bar{g} \right) / A = \left(\frac{4 + 3\bar{g}^2 - 2\bar{g}^3}{3}\pi + (A - \pi r_g^2)\bar{g} \right) / A$$

For this submerged case, R_q is:

$$2 R_q = \sqrt{\left(\int_0^{r_g} 2\pi x (\sqrt{1-x^2} + 1 - \bar{z})^2 dx + (A - \pi r_g^2)(\bar{z} - \bar{g})^2 \right) / A}$$

Figure 10 shows the conversion factors from ε to k_S as a function of relative glue thickness.

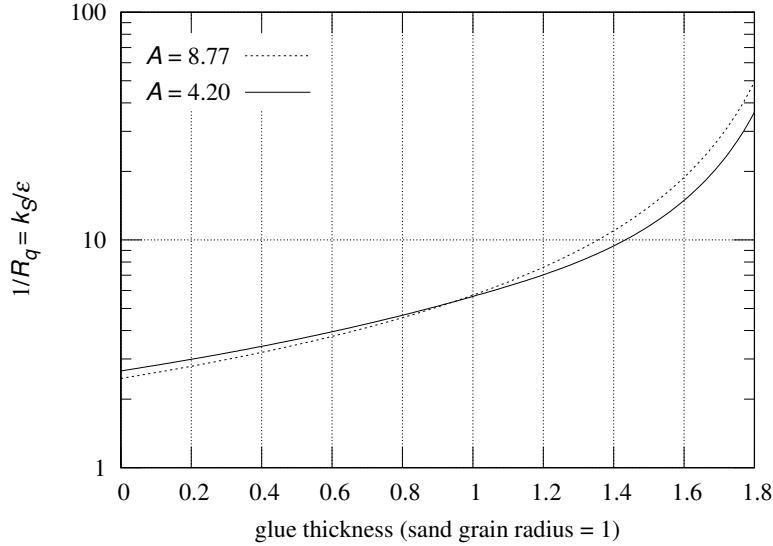


Figure 10 ε to k_S conversion factor vs. glue thickness and cell area A

In order to compare the Prandtl and Schlichting[1] formula (1) with formula (15) of present work, different k_S/ε conversion factors (having different relative glue thicknesses) must be used at large and small k_S values.

The unit cell area A for the larger grains is 4.2. With $L/\varepsilon = 150$, compare c_f for $L/k_S = L R_q/\varepsilon$ in Table 2 with $f_c = 0.0133$ calculated from equation (15):

\bar{g}	\bar{z}	$1/R_q$	L/k_S	c_f
0.00	1.25	2.66	56.4	0.0206
0.90	1.47	5.12	29.3	0.0266
1.00	1.50	5.64	26.6	0.0277

Table 2 RMS roughness R_q versus large-grain sand-roughness k_S

$f_c = 0.0133$ is out of the range of possible c_f values with $\bar{g} \geq 0$. However, the values of $c_f/2$ are within range of f_c .

A factor of 2 is introduced in the last step of Prandtl and Schlichting’s derivation[1]. While it is justified for the local coefficient of resistance, the reason for its presence in the total coefficient of resistance is difficult to discern through the many changes of variables.

In their example of the use of their formula, Mills and Hang[3] divide C_D by 2.

Half the c_f value from the $\bar{g} = 0.90$ row in Table 2 matches $f_c = 0.0133$.

Regardless of the etiology of this factor of 2, the Schlichting and Mills-Hang formulas in Figure 11 must be multiplied by 0.5 to bring them into the realm of plausibility.

The unit cell area for the smaller grains is 8.77. The largest pipe which Nikuradse tested had a diameter of 0.101 m. With a coating made from the smallest sand grain size (.01 cm), $L/k_S = 1014$ and the corresponding $f_c = 0.00696$. As before, there is no glue level $\bar{g} \geq 0$ whose c_f matches f_c , but half of c_f does match f_c at $\bar{g} = 0.99$ in Table 3.

\bar{g}	\bar{z}	$1/R_q$	L/k_S	c_f
0.00	0.60	2.46	411.4	0.0108
0.99	1.23	5.65	179.4	0.0138
1.50	1.57	13.95	72.7	0.0188

Table 3 RMS roughness R_q versus small-grain sand-roughness k_S

Afzal, Seena, and Bushra in *Turbulent flow in a machine honed rough pipe for large Reynolds numbers: General roughness scaling laws*[9] fit 5.333 for the RMS to sand-roughness conversion factor and 6.45 for the arithmetic-mean to sand-roughness conversion factor. The mean of the $1/R_q$ values 5.12 and 5.65 is 5.385, which is within 1% of 5.333 (and not close to 6.45). This is strong evidence that RMS height-of-roughness is the true metric for surface roughness.

The average of 5.385 and 5.333 is close to 5.36; 5.36 is used as the conversion factor for the Mills-Hang formula in Figure 11.

In *Skin-friction behavior in the transitionally-rough regime*[5], Flack, Schultz, Barros, and Kim measure skin-friction from grit-blasted surfaces. They write “The root-mean-square roughness height (k_{rms}) is shown to be most strongly correlated with the equivalent sand-roughness height (k_S) for the grit-blasted surfaces.”

Figure 11 shows that the corrected Mills-Hang formula (2) is nearly coincident with the equation (15) over the range $100 < L/\varepsilon < 1000$; so it is an improvement over Prandtl and Schlichting’s correlation (1). At $L/\varepsilon > 1000$, the inset in Figure 11 shows that both suffer from the scale error discussed in Section 2, growing to -13% and -18% relative to the equation (15) trace at $L/\varepsilon = 10^6$.

The 3 mm RMS roughness plate has an equivalent sand-roughness of 16 mm; $L/\varepsilon = 102$; $L/k_S = 19.0$

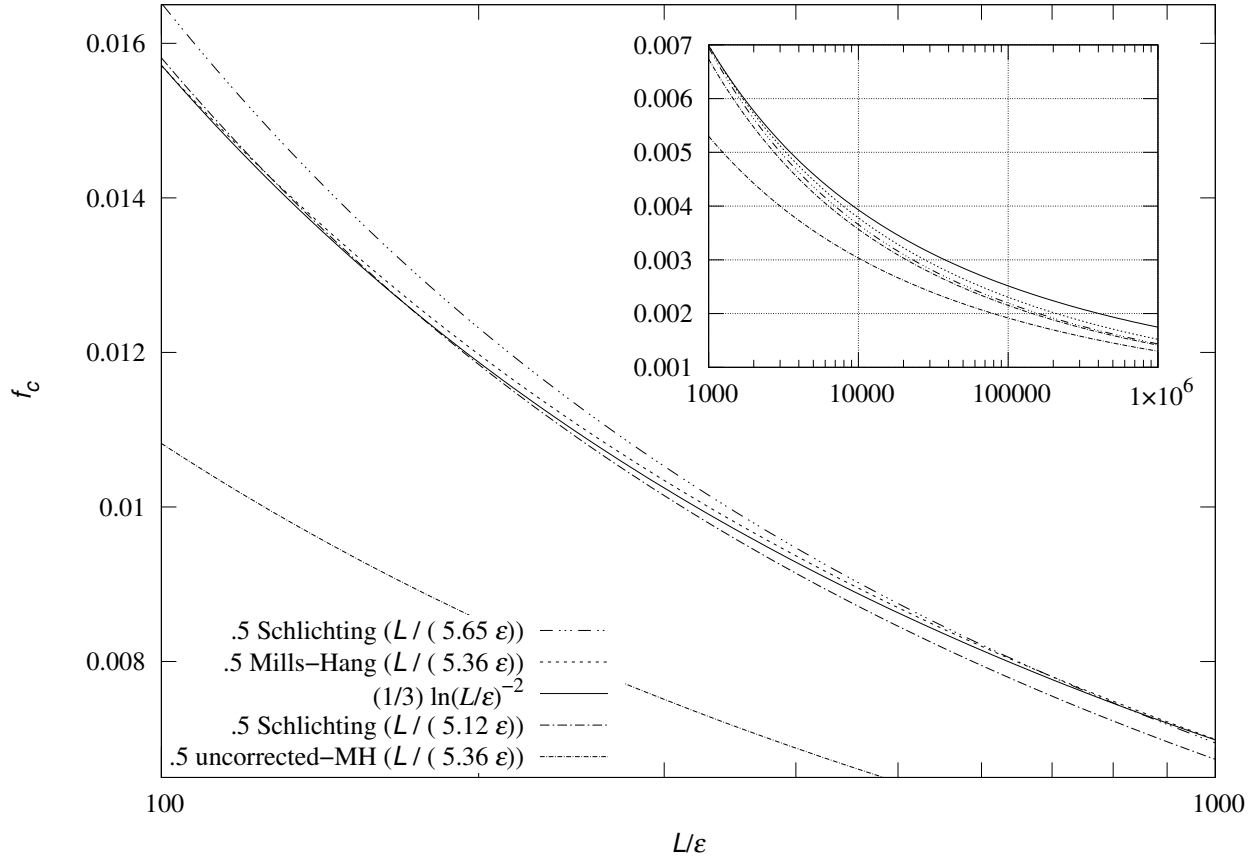


Figure 11 Fully rough (turbulent) friction coefficient

12. Roughness in Pipes

Applying self-similar roughness to pipe interiors is difficult because, while the isobaric plate environment allows roughness to grow proportionally to L , the boundary-layer runs out of room inside cylindrical pipes. Looking at roughness more generally may provide some insights.

The skin-friction coefficient of plate roughness being independent of Re is evidence that the monotonic/inflective variation in pipe skin-friction with Re is not due to some property of isotropic surface roughness. Commercial pipe interiors might well have longitudinal roughness different from circumferential roughness as a result of their manufacturing processes, for instance extrusion.

Assuming Nikuradse's sand-roughness samples had isotropic roughness, why aren't their Moody diagram traces flat?

The characteristic-length for pipe-flow is the diameter of the pipe; but the bulk flow is longitudinal. It is not clear that the longitudinal roughness should be measured against the same characteristic-length as the circumferential roughness. If the characteristic-lengths should be different, then pipe skin-friction should be formulated as a function of the circumferential and longitudinal roughness profiles (and Re) instead of a single surface roughness (and Re).

13. Conclusions

- For a flat surface with RMS height-of-roughness $\varepsilon \ll L$ which is producing turbulence:

$$f_c = \frac{1}{3 \ln^2(L/\varepsilon)} \quad \text{Nu} = \frac{\text{Re Pr}^{1/3}}{6 \ln^2(L/\varepsilon)}$$

- Unlike pipe interiors, these formulas hold for transitional-rough through fully rough flow regimes.
- Convection measurements of a bi-level isothermal plate having precisely 3 mm of RMS roughness match the convection correlation within 3% at Reynolds numbers from 5500 to 50000.
- These formulas are computed directly from RMS height-of-roughness, not converted into the untraceable sand-roughness unit.
- To convert between RMS height-of-roughness ε and sand-roughness k_S : $k_S \approx 5.12\varepsilon$ for Nikuradse's large sand-grain samples and $k_S \approx 5.65\varepsilon$ for his small sand-grain samples. The average of these two values with 5.333 from Afzal, Seena, and Bushra is $k_S \approx 5.36\varepsilon$.

Acknowledgments

The idea of self-similar roughness grew out of a discussion with Nina Koch about self-similarity in fluid-dynamics.

Thanks to John Cox for machining the bi-level plate. Thanks to Martin Jaffer and Roberta Jaffer for their assistance and problem-solving suggestions.

14. Nomenclature

Nu	= average Nusselt number (convection)
Pr	= fluid Prandtl number
Re	= Reynolds number of flow over plate
A	= area of square cell containing sphere sand grain (m ²)
C_D	= Mills and Hang friction coefficient
c_f	= Prandtl and Schlichting friction coefficient
f_c	= friction coefficient
\bar{g}	= height of glue (m)
$G(x, w)$	= Gray-code profile function
$j = \log_2 w$	= positive integer
k_S	= sand-roughness (m)
L	= plate characteristic-length (m)
n	= branching factor of profile roughness function
R_q	= dimensionless RMS height-of-roughness
r_g	= radius of glue opening exposing unit sphere
u	= fluid velocity (m/s)
u_R	= vertical roughness fluid velocity (m/s)
$w = 2^j$	= integer power of two
$W(x, w)$	= wiggliest integer self-similar profile function
$Y(x, w)$	= integer self-similar profile function
x, y	= distance (m)
$z(x)$	= profile roughness function (m)
$z(x, y)$	= surface roughness function (m)
\bar{z}	= mean height of roughness (m)
Z	= profile roughness function random variable (m)

Greek Symbols

ϵ = RMS profile height-of-roughness (m)
 ε = RMS surface height-of-roughness (m)
 ρ = fluid density (kg/m³)
 τ = fluid shear stress (N/m²)

15. References

- [1] L. Prandtl and H. Schlichting. *The Resistance Law for Rough Plates*. Translation (David W. Taylor Model Basin). Navy Department, the David W. Taylor Model Basin, 1934. Translated 1955 by P.S. Granville.
- [2] Hermann Schlichting, Klaus Gersten, Egon Collaborateur. Krause, Herbert Collaborateur. Oertel, and Katherine Mayes. *Boundary-layer theory*. Springer, Berlin, Heidelberg, Paris, 2000. Corrected printing 2003.
- [3] A. F. Mills and Xu Hang. On the skin friction coefficient for a fully rough flat plate. *J. Fluids Eng*, 105(3):364–365, 1983.
- [4] M. M. Pimenta, R. J. Moffat, and W. M. Kays. *The Turbulent Boundary Layer: An Experimental Study of the Transport of Momentum and Heat with the Effect of Roughness*. Department of Mechanical Engineering, Stanford University, 1975.
- [5] Karen A Flack, Michael P Schultz, Julio M Barros, and Yechan C Kim. Skin-friction behavior in the transitionally-rough regime. *International Journal of Heat and Fluid Flow*, 61:21–30, 2016.
- [6] Mitchell G. Newberry and Van M. Savage. Self-similar processes follow a power law in discrete logarithmic space. *Phys. Rev. Lett.*, 122:158303, Apr 2019.
- [7] A. Jaffer. Convection measurement apparatus and methodology, 2019. [Online; accessed 20-June-2019].
- [8] A. Jaffer. Turbulent mixed convection from an isothermal plate, 2019. [Online; accessed 13-June-2019].
- [9] Noor Afzal, Abu Seenaa, and A. Bushra. Turbulent flow in a machine honed rough pipe for large reynolds numbers: General roughness scaling laws. *Journal of Hydro-environment Research*, 7(1):81–90, 2013.